Available online at www.sciencedirect.com

SciVerse ScienceDirect

Ceramics International 38 (2012) 6273–6279

CERAMICS INTERNATIONAL

www.elsevier.com/locate/ceramint

Effect of sintering atmosphere and lithium ion co-doping on photoluminescence properties of $NaCaPO_4:Eu^{2+}$ phosphor

Bhaskar Kumar Grandhe[a], Vengala Rao Bandi[a], Kiwan Jang[a,*], Ho-Sueb Lee[a], Dong-Soo Shin[b], Soung-Soo Yi[c], Jung-Hyun Jeong[d]

[a]*Department of Physics, Changwon National University, Changwon, South Korea*
[b]*Department of Chemistry, Changwon National University, Changwon, South Korea*
[c]*Department of Photonics, Silla University, Busan, South Korea*
[d]*Department of Physics, Pukyong National University, Busan, South Korea*

Received 3 April 2012; received in revised form 27 April 2012; accepted 27 April 2012
Available online 9 May 2012

Abstract

This paper reports on the photoluminescence properties of $Na_{1-y}Li_yCa_{1-x}PO_4:_xEu^{2+}$ phosphors synthesized by a solid state reaction method. The prepared phosphors have been thoroughly characterized by means of X-ray diffraction (XRD), Field-emission scanning electron microscopy (FE-SEM), Fourier transform infrared spectrum (FTIR), Raman spectrum, Thermo gravimetric and differential thermal analysis (TG–DTA) and photoluminescent spectral measurements. The structure of $Na_{1-y}Li_yCa_{1-x}PO_{4:x}Eu^{2+}$ phosphors were found to be orthorhombic in nature with a sphere-like morphology and having the particle size in micrometer range. The excitation spectra of $NaCaPO_4:Eu^{2+}$ phosphors revealed a broad excitation band having its maximum intensity at 373 nm and ranging from 250 m to 450 nm. Incidentally, it matches well with the ultraviolet (UV) radiation of light-emitting diodes (LEDs). Upon 373 nm excitation, these phosphors exhibited intense bluish-green emission band centered at 505 nm. The effect of sintering atmospheres and co-doping of lithium ions on the photoluminescence properties of the $NaCaPO_4:Eu^{2+}$ phosphors were studied and explained suitably. The obtained results indicate that the prepared $NaCaPO_4:Eu^{2+}$ phosphors are promising bluish-green candidates for the phosphor-converted white LED applications.

Keywords: A: Sintering; B: Nanocomposites; C: Optical Properties

1. Introduction

With fossil fuels being in short supply and as global climate change is deteriorating each year; our standard of living can only be maintained by significant improvements in energy efficiency. Large amounts of energy are being consumed for the sake of lighting and displays. Since the realization of GaN-based light emitting diodes (LEDs), more and more interest has been focused on white LED phosphors, as it has many advantages like long lifetime, high rendering index, high luminosity efficiency, and a concurrent reduction in environment pollution over the incandescent and fluorescent lamps [1–3].

The generation of white light through a combination of an ultraviolet or blue-emitting chip and phosphors as solid-state lighting sources has attracted considerable interest. The first commercial phosphor-converted white light-emitting diodes (pc-WLEDs) has been produced by the combination of blue LED with yellow-emitting cerium doped yttrium aluminum garnet (YAG:Ce) phosphor. However, this approach suffers from the disadvantages like thermal quenching, poor color rendition and narrow visible range [4,5]. Hence in recent days, much attention has been focused on the generation of white light, through a combination of red, green and blue phosphors with UV or near-UV (365–410 nm) LED. From the perspective of efficiency and good color render index, red/green/blue color emitting phosphors having their prominent excitation wavelengths in range of 350–410 nm are very important [6,7]. Currently, the commonly used green-emitting

*Corresponding author. Tel.: +82 552133425.
E-mail address: kwjang@changwon.ac.kr (K. Jang).

0272-8842/$36.00 © 2012 Elsevier Ltd and Techna Group S.r.l. All rights reserved.
http://dx.doi.org/10.1016/j.ceramint.2012.04.082

phosphors for white LEDs are sulfide phosphors, such as ZnS:Cu, Al and $SrGa_2S_4:Eu^{2+}$, which show poor chemical stabilities against humidity and strong degradation upon LED chip pumping [8,9]. Therefore, it is vital to develop new green phosphors with comparatively modest synthesis method and which can exhibit superior luminescence performance than sulfides.

The emission and absorption spectra of Eu^{2+} usually consist of broad bands due to transitions between the $^8S_{7/2}$ ($4f^7$) ground state and the crystal field components of the $4f^65d$ excited state configuration. Since the involved 5d orbitals are external, the position of these energy levels and consequently the wavelength of excitation and emission bands strongly depend on the host crystal. The absorption spectrum in UV region and the broad emission spectrum in UV-infrared region can be influenced by the crystal-lattice environment of the Eu^{2+} ions. Through appropriate host selection, the luminescence of Eu^{2+} can be adjusted with different crystal field splitting of the 5d band, which can allow a range of color temperatures that are suitable for white LEDs [10,11].

Orthophosphate phosphors exhibit an excellent thermal and hydrolytic stability, which are primary requirements of an efficient host material. Among all, $NaCaPO_4$ (NCP) host matrix has lower synthesis temperature and higher physical and chemical stability. It also possesses an appropriate structure containing a rigid three-dimensional network of tetragonal PO_4 groups [12–14]. In general, most of the commercial phosphors are prepared by solid-state reaction method. Hence in the present study, we adopted the solid state reaction method to prepare and analyze the photoluminescent properties of $NaCaPO_4:Eu^{2+}$ phosphors. We have also thoroughly investigated the effect of sintering atmosphere and lithium ion co-doping in order to obtain best possible bluish green emission from the $NaCaPO_4:Eu^{2+}$ phosphors. For the optimized phosphor sample, XRD, SEM, FTIR and Raman spectral profiles were also recorded and analyzed.

2. Experimental procedure

$Na_{1-y}Li_yCa_{1-x}PO_4{:}xEu^{2+}$ phosphors were prepared by a conventional solid state reaction method by sintering the phosphor precursor at 850 °C in different sintering atmospheres. Analytical reagent grade high pure Na_2CO_3, Li_2CO_3, $CaCO_3$, $NH_4H_2PO_4$ and Eu_2O_3 chemicals were weighed in requisite proportions and grounded in an agate mortar with methyl alcohol to obtain homogeneous mixture. Differential thermal analysis (DTA) and thermo gravimetric analysis were employed to determine the suitable heat treatment procedure. The mixture was kept in an alumina crucible and sintered in different atmospheres like air, oxygen (O_2), argon (Ar) and N_2H_2 (95% N_2 and 5% H_2) by a three-step heating process (200 °C for 2 h, 700 °C for 1 h, and 850 °C for 3 h) to obtain Eu^{2+}:$NaCaPO_4$ phosphor. Finally, the samples are grounded into fine powder for their characterization and analysis.

The crystal structure of the prepared phosphors was investigated by using X-ray powder diffraction (Philips X'pert, MPD 3040, Westborough, MA) over the 2θ range from 20° to 60°. The morphology of the powder phosphors was observed by employing field-emission scanning electron microscope (FE-SEM) (Tescan, MIRA IILMH, Brno, Czech Republic). FTIR spectrum of the phosphor sample was recorded on a Jasco FTIR-200 E spectrometer with KBr pellet technique from 4000 cm^{-1} to 400 cm^{-1}. Raman spectrum was recorded by using a high resolution NRS-3300 laser Raman spectrophotometer (JASCO) system equipped with a DPSS green diode laser (532 nm) as the excitation source. Emission and excitation spectra were measured using a Shimadzu, RF-5301PC spectrofluorophotometer (Kyoto, Japan). The TG–DTA analysis were performed by using the thermal analyzer system (Model: TA 5000/SDT 2960 DSC Q10) in a alumina crucible at heating rate 10 °C/min, from 20 °C to 1000 °C at N_2 gas atmosphere. All spectroscopic measurements were performed at room temperature.

3. Results and discussion

Fig. 1 shows the XRD patterns of $NaCa_{0.99}PO_4:Eu_{0.01}$ and $Na_{0.96}Li_{0.04}Ca_{0.99}PO_4:Eu_{0.01}$ phosphors sintered in different atmospheric conditions. The XRD patterns of all the prepared phosphors are in good agreement with the Joint Committee on Powder Diffraction Standards data (JCPDS) card bearing the number 29-1193, indicating that the incorporated dopant ions and the sintering atmosphere has not caused any significant changes to the orthorhombic crystal structure of $NaCaPO_4$ matrix. Fig. 2 shows the FE-SEM image of $Na_{0.96}Li_{0.04}Ca_{0.99}PO_4:Eu_{0.01}$ phosphor which is sintered initially in argon and later in N_2H_2 atmosphere at 850 °C. Here after, for the sake of clear understanding and reader's convenience, this sintering criterion will be mentioned as (Ar–N_2H_2). The obtained micrograph shows that the particles are agglomerated and

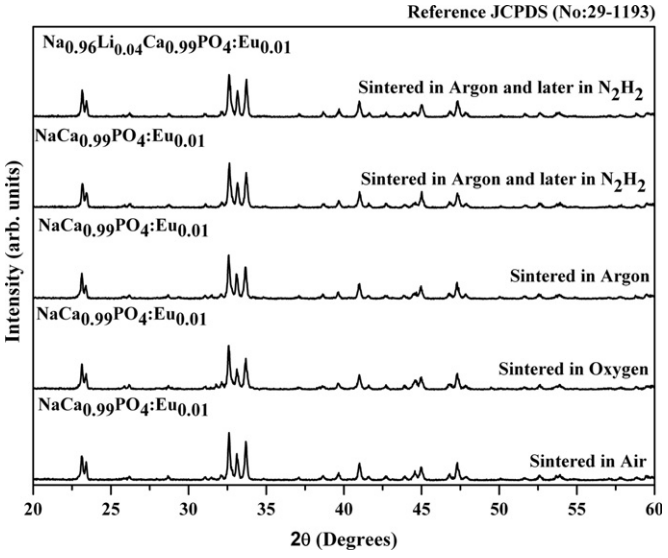

Fig. 1. XRD patterns of $NaCaPO_4:Eu^{3+}$ phosphors sintered in different atmospheres.

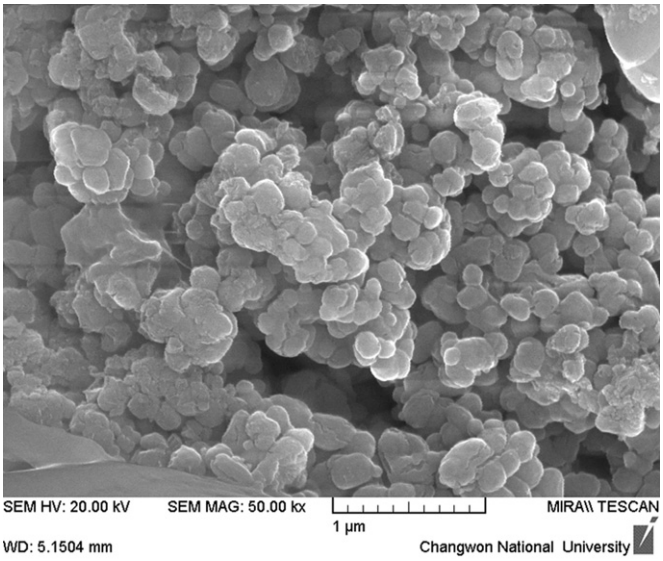

Fig. 2. SEM photograph of $NaCaPO_4:Eu^{3+}$ phosphors sintered in argon initially and later in N_2H_2 atmosphere.

possess a sphere like morphology. The approximate size of those particles might be in micrometer range which is a suitable size for fabrication of SSL devices. From literature also it is noticed that the crystalline powder in micrometer dimension will find more applications as these micro crystalline phosphors can result in high luminescent intensities [15]. No significant diversifications were noticed in the Fe-SEM images of other phosphor samples.

FT-IR spectra of the $NaCa_{0.99}PO_4:Eu_{0.01}$ and $Na_{0.96}Li_{0.04}Ca_{0.99}PO_4:Eu_{0.01}$ phosphors sintered in Ar and Ar–N_2H_2 atmospheres, respectively, are shown in Fig. 3(a). Usually, the IR absorption band of $(PO_4)^{3-}$ has two regions of $1120-940\ cm^{-1}$ and $650-540\ cm^{-1}$. The phosphate units in Fig. 3(a) are characterized by two broad IR absorption bands centered near $1050\ cm^{-1}$ and $570\ cm^{-1}$ that are assigned to the stretching and bending vibration modes of the $(PO_4)^{3-}$ units, respectively. However, we noticed some insignificant bands near $1636\ cm^{-1}$and $3440\ cm^{-1}$ that are associated to the OH content absorbed at the powder surface when the sample was in contact with the environment during the measurement process [16–18]. Fig. 3(b) shows the Raman spectra of the $NaCa_{0.99}PO_4:Eu_{0.01}$ and $Na_{0.96}Li_{0.04}Ca_{0.99}PO_4:Eu_{0.01}$ phosphors sintered in Ar and Ar–N_2H_2 atmospheres, respectively. $(PO_4)^{3-}$ free ions have four basic vibration modes: ν_1(A1) of P–O symmetric stretching vibration, ν_2(E) of PO_2 symmetric bending vibration, ν_3(F2) of PO asymmetric stretching vibration and ν 4(F2) of PO_2 asymmetric bending vibration in the $(PO_4)^{3-}$ tetrahedron. In the crystal structure, $(PO_4)^{3-}$ vibration may have some changes due to disorder of the local point symmetry and anion O_2^- ions. The band at $967\ cm^{-1}$ is assigned to $\nu_1(PO_4)^{3-}$ symmetric stretching vibration, 429icm^{-1} and $454\ cm^{-1}$ to $\nu_2(PO_4)^{3-}$ bending vibrations, 1048 and 1027,cm^{-1} to $\nu_3(PO_4)^{3-}$ antisymmetric stretching vibrations and $591\ cm^{-1}$ to $\nu_4(PO_4)^{3-}$ bending vibration, respectively. All the assignments made above are in good agreement with the earlier published reports [18–20].

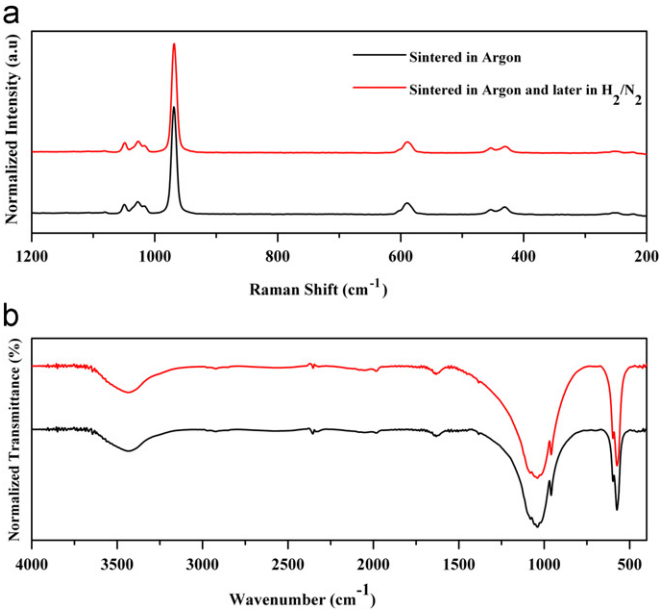

Fig. 3. FTIR and Raman spectra of $NaCaPO_4:Eu^{3+}$ phosphors (a) sintered in argon initially and later in N_2H_2 atmosphere (b) sintered in argon atmosphere.

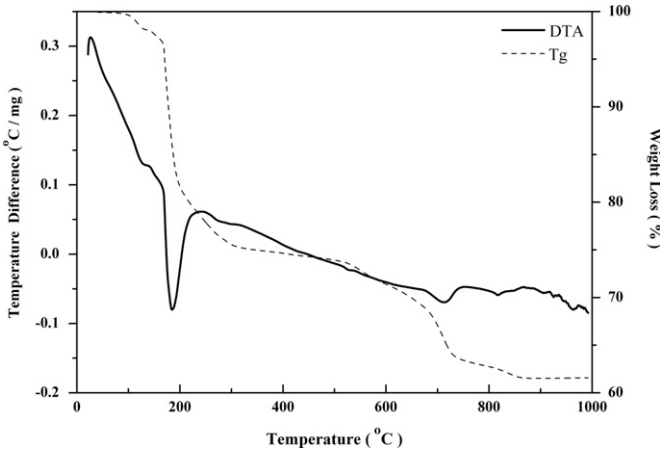

Fig. 4. Tg–DTA profile of $NaCa_{0.99}PO_4:Eu_{0.01}$ phosphor precursor.

The TG–DTA profile of $NaCa_{0.99}PO_4:Eu_{0.01}$ phosphor precursor is shown in Fig. 4. In the temperature range from 20 °C to 200 °C, the sample shows both exothermic and endothermic peaks in the DTA curve, which is consistent with the first weight loss. These observations can be attributed to the decomposition of NH_3, H_2O and the organic species that were used during the grinding process of starting chemicals. The second weight loss in the range of 200 °C and 700 °C was due to the degradation of any other residual organic material from the precursor which is also accompanied by the removal of CO_2 gases that arouses from the starting chemicals [21,22]. Upon increasing the temperature up to 1000 °C, a solid state reaction occurs amongst those precursor chemicals and peaks observed in the DTA curve confirm such a reaction. TG curve indicates a total weight loss of nearly 38% when

the temperature is raised from 30 °C to 1000 °C. No significant weight loss has been observed in the TG curve, when the temperature was raised beyond 800 °C.

Photoluminescent property of any phosphor will be strongly related with the valence state of its activator or dopant ion. It is well known, some kinds of reducing agents, such as H_2/CO, are needed to reduce the Eu^{3+} to Eu^{2+} in a solid state compound. But in some special cases, this reduction could be thermally achieved even when sintered in a non reducing atmosphere [23]. In the present investigation, we observed the reduction phenomenon of Eu^{3+} to Eu^{2+} in $NaCaPO_4$ compound when sintered in a non reducing atmosphere of pure argon. However, from the emission spectral features of phosphor sample sintered in Argon atmosphere, we noticed that certain quantity of europium ions still existing in its trivalent state. Fig. 5 shows the PL excitation and emission spectra of $NaCa_{0.99}PO_4:Eu^{2+}_{0.01}$ phosphor sintered in pure argon atmosphere. The excitation spectra were recorded by using 595 nm and 505anm as the emission wavelengths. Both the excitation spectra reveal a broad band, extending from 250 m to 450hnm reaching its maximum value at 373 nm. This intense and broad band can be attributed to the 4f–5d transition of Eu^{2+} ions. The prominent excitation band located at 373 nm indicates that the $NaCa_{0.99}PO_4:Eu^{2+}_{0.01}$ phosphor is very much suitable for a color converter using UV light as the primary light source. It can be used as a green phosphor excited by UV LED chip and mixed with other color emission phosphors to obtain white light. In the case of the excitation spectra monitored with 595 nm excitation, it shows an unique excitation band at 395 nm ($^7F_0 \rightarrow {}^5L_6$) indicating the possible existence of trivalent state of europium ions in the sintered sample. Fig. 5 also shows the emission spectra of $NaCaPO_4:Eu^{2+}$ phosphors sintered in pure argon atmosphere and measured with 373 nm and 395anm as the excitation wavelengths. Both the emission spectral profiles were dominated by the broad

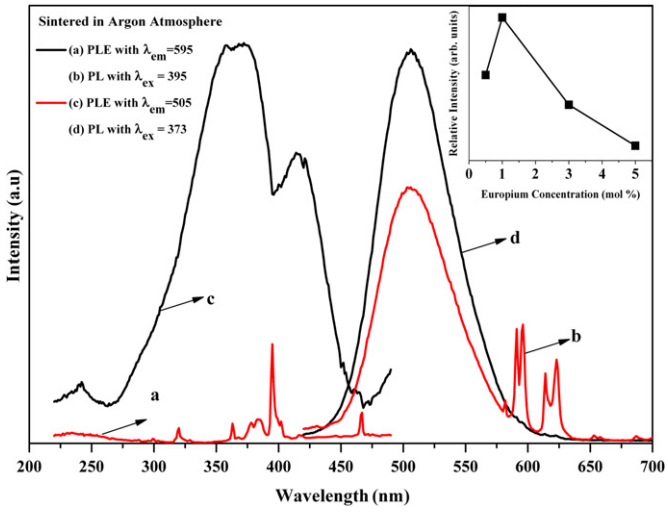

Fig. 5. PL excitation and emission spectra of $NaCa_{0.99}PO_4:Eu_{0.01}$ phosphors sintered in argon atmosphere. Inset figure shows the graph between dopant ion concentration and emission intensity.

and intense emission band reaching its maximum value at 505 nm and that can be ascribed to the $4f^65d \rightarrow {}^7({}^8S_{7/2})$ transition of Eu^{2+} ions [24]. It corresponds to the allowed f–d transition of Eu^{2+}. The 5d energy level of Eu^{2+} and the lower level of 4f state overlap, so the electron of 4f state can be excited to 5d state. The broad luminescence of Eu^{2+} is due to $^4f_65d_1 \rightarrow {}^4f_7$ transitions, which is an allowed electrostatic dipole transition [10]. Nevertheless, the 5d state is easily affected by the crystal field; that is to say, different crystal fields can split the 5d state in different way. This makes Eu^{2+} emitting different wavelength light in different crystal fields and the emission spectrum can vary from the ultraviolet to the red region [25]. Besides, in the emission spectra also we observed some characteristic emission bands at 595nm ($^5D_0 \rightarrow {}^7F_1$), 621nm ($^5D_0 \rightarrow {}^7F_2$), 653 nm ($^5D_0 \rightarrow {}^7F_3$) and 687 nm ($^5D_0 \rightarrow {}^7F_4$) relating to Eu^{3+} state when recorded with an excitation wavelength of 395 nm ($^7F_0 \rightarrow {}^5L_6$) [26]. The inset of Fig. 5 shows the graph between dopant ion concentration and emission intensity of the phosphors samples that were sintered in argon atmosphere. It is evident from the figure that the 1 mol% concentration is displaying better emission profile than the other dopant concentrations. The emission intensity increases with increasing of europium ion concentration, and reaches the maximum value at about 1 mol%. Concentration quenching phenomenon occurs, when the europium ion concentration was increased beyond 1 mol%.

According to earlier published reports, there are four conditions that are essential to reduce Eu^{3+} to Eu^{2+} in solid state compounds when prepared in a non reducing atmosphere [23]. They are as follows: (1) No oxidizing ions should be present in the host compounds, (2) The trivalent Eu^{3+} ion should replace a divalent cation in the host compound, (3) The substituted cation should posses a similar radius to the divalent Eu^{2+} ion, (4) The host compound should posses an appropriate structure, based upon tetrahedral anion groups (BO_4, SO_4, PO_4, or AlO_4). We examined the reduction of Eu^{3+} to Eu^{2+} in the $NaCaPO_4$ compound based on the four essential conditions mentioned above. An acceptable percentage difference in ion radii between doped and substituted ions must not exceed 30% [27]. The calculations of the radius percentage difference between the doped ions (Eu^{3+}) and the possible substituted ions (Ca^{2+} and P^{5+}) in $NaCaPO_4$ are analyzed based on the following equation:

$$Dr = 100 \times [Rm(CN) - Rd(CN)]/Rm(CN)$$

where Dr is the radius percentage difference, CN is the coordination number, Rm(CN) is the radius of the host cation, and Rd(CN) is the radius of doped ion [23,28]. Taking the above formula into consideration and calculating those values for the possible substituted ions (Ca^{2+} and P^{5+}), the value of Dr between Eu^{3+} and Ca^{2+} on eight coordinated sites was found to be 4.8%, while the value of Dr between Eu^{3+} and P^{5+} is −457.05%. Hence it is interpreted that, europium ions will substitute the Ca

sites. On the basis of the R.D.Shannon effective ionic radii of cations [29], it is clear that the Eu^{3+} (1.066 Å) ion prefer to substitute the Ca^{2+} ions among the Ca^{2+} (1.12 Å) and P^{5+} (0.17 Å) because of their similar ionic radii. The above analyses showed that conditions (2) and (3) were satisfied. In $NaCaPO_4$ compound there exits no oxidizing ions, which satisfy condition (1). Besides, host compound has an appropriate structure, based upon tetrahedral anion groups (PO_4), as evident from obtained FTIR spectrum (Fig. 3) of the prepared sample and hence the condition (4) is also satisfied. Therefore, all the four conditions which are essential for the reduction of Eu^{3+} to Eu^{2+} in $NaCaPO_4$ compound when sintered in a non reducing atmosphere are satisfied.

Further, the mechanism involved in the reduction of europium ions in the $NaCaPO_4$ matrix can be also explained as follows: From a chemistry point of view, the reduction of Eu^{3+} to Eu^{2+} reaction needs an electron anyway. When trivalent Eu^{3+} ions are doped in to $NaCaPO_4$ matrix, they will replace the divalent Ca^{2+} ions. To keep the electro neutrality of the compound, two Eu^{3+} ions would substitute for three Ca^{2+} ions. Therefore, two positive defects of $[Eu_{Ca}]^*$ and one negative Ca^{2+} vacancy of $[V_{Ca}]'$ would be created by each substitution for every two Eu^{3+} ions in the compound. By thermal stimulation, electrons of the $[V_{Ca}]'$ vacancies would be then transferred to doped Eu^{3+} ions and reduce them to their Eu^{2+}. Hence, it is assumed that the more electrons carried by negative defects were created; the more Eu^{3+} ions would be reduced to Eu^{2-} ions. Owing to these reasons of charge compensation, Eu^{3+} was subsequently intrinsically reduced to Eu^{2+}. The rigid three-dimensional network of tetragonal PO_4 groups can surround and isolate the produced divalent europium ions from reacting with oxygen. Thus, necessary existence of defect electrons and the anion structures of compounds play an important role in the transfer process of defect electrons to the doped RE^{3+} ions by thermal stimulation [30]. On the whole, it can be understood that, when the $NaCaPO_4:Eu^{2+}$ phosphor was sintered in pure argon atmosphere, most of the europium ions could able to uphold its divalent state even when the samples are sintered in a non-reducing atmosphere. However, there exists certain quantity of europium ions in trivalent state as evident from the observed characteristic eu^{3+} emission and excitation bands in Fig. 5.

Nevertheless for further assessment and also to enhance the PL efficiency of the $NaCaPO_4:Eu^{2+}$ phosphors, we have investigated the effect of various sintering criterions like sample sintered in air was cooled to room temperature and later it was again sintered in N_2H_2 atmosphere at 850 °C for 3 h. (Here after this sintering criterion will be labeled as Air-N_2H_2). Similarly, the other sintering criterions namely O_2–N_2H_2, Ar–N_2H_2 were also adopted. Fig. 6 shows the emission spectra of all the prepared phosphor samples that were measured with 373 nm and 395 nm excitation wavelengths. We can clearly notice that the Ar–N_2H_2 sintering criterion is exhibiting superior green

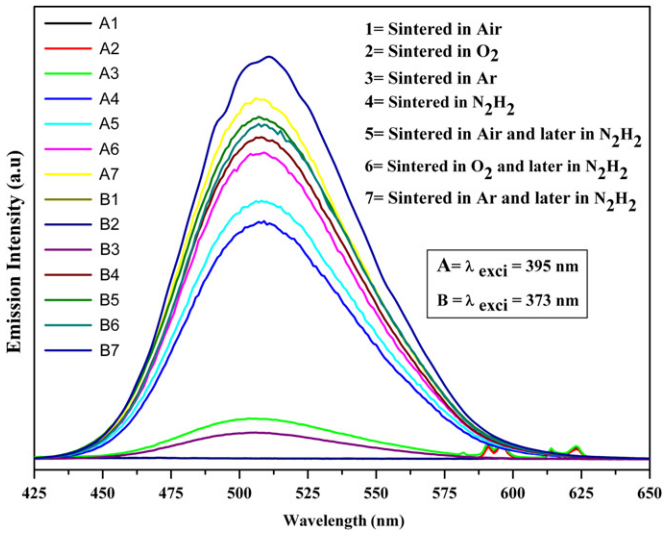

Fig. 6. PL emission spectra of $NaCa_{0.99}PO_4:Eu_{0.01}$ phosphors (A) with $\lambda_{exc\ i}$=395 nm (B) with $\lambda_{exc\ i}$=373 nm and sintered in different atmospheric conditions.

emission than all other adopted sintering criterions. It can be understood from the A3 emission spectral profile of Fig. 6 that even though majority of the Eu^{3+} ions could able to reduce to divalent state when sintered in a non-reducing argon atmosphere, still there exist a modest amount of europium ions in its trivalent state. Hence, when the same phosphor sample was again sintered in a reducing atmosphere of 95% N_2 and 5% H_2 could able to exhibit superior green emission than all other phosphor samples that were shown in Fig. 6. The emission intensity of Ar–N_2H_2 criterion has increased almost ten times when compared with that of sample sintered in pure Argon atmosphere.

Several groups have investigated the effect of lithium ion incorporation on the phosphor efficiency. Such studies revealed that the photoluminescent efficiency of those phosphors was enhanced remarkably by the incorporation of Li ions [31,32]. For this reason, in our present investigation we have also incorporated Li ions in place of Na ions to study its influence on the photoluminescence property of the $NaCaPO_4:Eu^{2+}$ phosphor by adopting the Ar–N_2H_2 sintering criterion. We observed a drastic enhancement in the photoluminescence efficiency of $NaCa_{0.99}PO_4:Eu_{0.01}$ phosphor when lithium ions were incorporated in place of Na ions. We have further optimized the lithium concentration and its emission spectral features were shown in Fig. 7. Among all the Li co-doped samples, the $Na_{1-y}Li_yCa_{0.99}PO_4:Eu_{0.01}$ phosphor containing 4 mol% of lithium (y=0.04) is exhibiting superior luminescence efficiency when compared with other samples. Moreover, we have done XRD characterization to analyze the possible structural explanation for this. It was found that diffraction patterns of phosphors with and without lithium ions are all the same. The evident change of the emission intensity is due to the differences of the ionic radii of alkali metal ions. The alkali metal ions of Li^+, Na^+ and

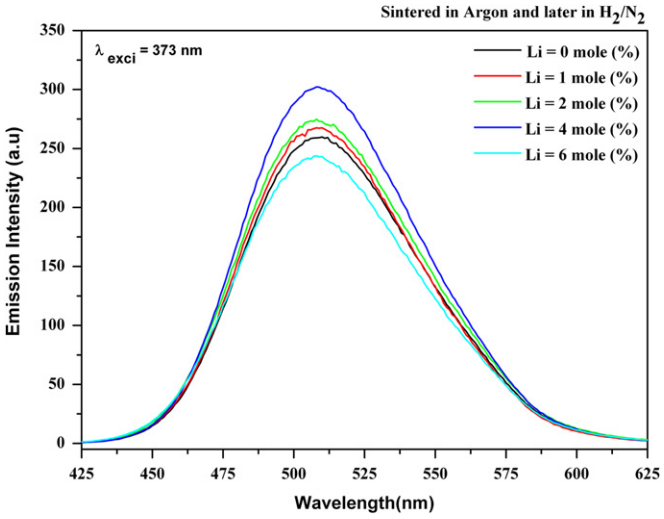

Fig. 7. PL emission spectra of $Na_{1-y}Li_yCa_{0.99}PO_4:Eu_{0.01}$ phosphors sintered in argon initially and later in N_2H_2 atmosphere with varying lithium ion concentrations.

K^+ have the valence electronic configurations of noble gases. The alkali metal ions have ionic radii in the increasing order of $Li^+ < Na^+ < K^+$. The difference in the ionic radii would probably give rise to diversity in the sub lattice structure around the luminescent center ions. This in turn influences the spin–orbit coupling and the crystal field of europium ions. Thus, the relative emission intensity of the phosphors co-doped with lithium is strongly enhanced as the coordination conditions of europium ions are influenced due to the change in distances between Eu and O [33].

In general, color is represented by means of color coordinates. The chromaticity diagram established by the Commission Internationale de l'Eclairage (CIE) in 1931 is a two dimensional graphical representation of any color perceivable by the human eye on an *x*–*y* plot. Hence, in our present work, the chromaticity coordinates of optimized $Na_{0.96}Li_{0.04}Ca_{0.99}PO_4:Eu_{0.01}$ phosphor has been calculated and it is having a numerical value of (0.162, 0.557).

4. Conclusions

In summary, conventional solid-state route was adopted to prepare a series of phosphate phosphors ($Na_{1-y}Li_yCa_{1-x}PO_4:Eu_x$) sintered in various criterions and their photoluminescent properties were studied. The prepared phosphors can be excited very efficiently by near-ultraviolet (*n*-UV) light irradiation, exhibiting bright bluish-green emission. For the first time, we have noticed reduction of Eu^{3+} to Eu^{2+} in $NaCaPO_4$ compound sintered in a non reducing atmosphere of pure Argon. This abnormal reduction was explained appropriately by a charge compensation mechanism. The tetrahedral PO_4 anion groups of the NaCaPO4 compound played a role of electron transfer in the reduction process of Eu^{3+} to Eu^{2+} in non-reducing atmosphere. Sintering criterion greatly affects the photoluminescent efficiency of the $NaCaPO_4:Eu^{2+}$ phosphor. Stronger bluish-green emission was further obtained with the addition of lithium ion, which is of great value owing to its lower cost than the rare earth ions. Based on the obtained results, we suggest that the optimized $Na_{0.96}Li_{0.04}Ca_{0.99}PO_4:Eu_{0.01}$ phosphor as a promising candidate for the fabrication of phosphor converted white LED's.

Acknowledgments

This work was supported by the Priority Research Centers Program through the National Research Foundation of Korea funded by the Ministry of Education, Science and Technology (NRF-2010–0029634) and also this work was partially supported by the National Research Foundation of Korea funded by the Korean government (NRF-2010–0023034).

References

[1] C.C. Lin, R. Liu, Advances in phosphors for light-emitting diodes, Journal of Physical Chemistry Letters 2 (2011) 1268–1277.
[2] X. Zhang, Z. Lu, F. Meng, F. Lu, L. Hu, X. Xu, C. Tang, A yellow-emitting $Ca_3Si_2O_7:Eu^{2+}$ phosphor for white LEDs, Materials Letters 66 (2012) 16–18.
[3] Y. Lu, G. Shi, Q. Zhang, H. Wang, Y. Li, Photoluminescence properties of Eu^{2+} and Mg^{2+} co-doped $CaSi_2O_2N_2$ phosphor for white light LEDs, Ceramics International 38 (2012) 3427–3433.
[4] Y. Chang, C. Liang, S. Yan, Y. Chang, Synthesis and photoluminescence characteristics of high color purity and brightness $Li_3Ba_2Gd_3(MoO_4)_8:Eu^{3+}$ red phosphors, Journal of Physical Chemistry C 114 (2010) 3645–3652.
[5] V.R. Bandi, B.K. Grandhe, K. Jang, H. Lee, S. Yi, J. Jeong, Single-phased and emission-tunable $CaLa_{2-x}Eu_xZnO_5$ phosphors with blue light excitation for WLEDs, Functional Materials Letters 4 (1) (2011) 79–82.
[6] L. Liu, R. Xie, N. Hirosaki, Y. Li, T. Takeda, C. Zhang, J. Li, X. Sun, Crystal structure and photoluminescence properties of red-emitting $Ca_9La_{1-x}(VO_4)_{7:x}Eu^{3+}$ phosphors for white light-emitting diodes, Journal of the American Ceramic Society 93 (12) (2010) 4081–4086.
[7] V.R. Bandi, B.K. Grandhe, K. Jang, H. Lee, S. Yi, J. Jeong, Citric based sol–gel synthesis and photoluminescence properties of undoped and Sm^{3+} doped $Ca_3Y_2Si_3O_{12}$ phosphors, Ceramics International 37 (2011) 2001–2005.
[8] X. Zhang, J. Zhang, R. Wang, M. Gong, Photo-physical behaviors of efficient green phosphor $Ba_2MgSi_2O_7:Eu^{2+}$ and its application in light-emitting diodes 93 (5) (2010) 1368–1371 Journal of the American Ceramic Society 93 (5) (2010) 1368–1371.
[9] V.R. Bandi, B.K. Grandhe, K. Jang, H. Lee, D. Shin, S. Yi, J. Jeong, Citric based sol–gel synthesis and luminescence characteristics of $CaLa_2ZnO_5:Eu^{3+}$ phosphors for blue LED excited white LEDs, Journal of Alloys and Compounds 512 (2012) 264–269.
[10] W.J. Park, Y.H. Song, D.H. Yoon, Synthesis and luminescent characteristics of $Ca_{2-x}Sr_xSiO_4:Eu^{2+}$ as a potential green-emitting phosphor for near UV-white LED applications, Materials Science and Engineering B 173 (2010) 76–79.
[11] V.R. Bandi, B.K. Grandhe, K. Jang, S. Kim, D. Shin, Y. Lee, J. Lim, T. Song, Luminescent properties of a new green emitting Eu^{2+} doped $CaZrSi_2O_7$ phosphor for WLED applications, Journal of Luminescence 131 (2011) 2414–2418.
[12] S. Zhang, X. Wu, Y. Huang, Photoluminescence and thermal stability of Eu^{2+}-activated $LiCaPO_4$ phosphors for white light-

emitting diodes, International Journal of Applied Ceramic Technology 8 (4) (2011) 734–740.
[13] N. Guo, Y. Song, H. You, G. Jia, M. Yang, K. Liu, Y. Huang, H. Zhang, Optical properties and energy transfer of $NaCaPO_4:Ce^{3+},Tb^{3+}$ phosphors for potential application in light-emitting diodes, European Journal of Inorganic Chemistry (2010) 4636–4642.
[14] K.N. Shinde, S.J. Dhoble, A. Kumar, Photoluminescence studies of $NaCaPO_4$:RE (RE=Dy^{3+}, Mn^{2+} or Gd^{3+}), Physica B 406 (2011) 94–99.
[15] B. Yan, C. Wang, Synthesis and luminescence properties of $REAl_3(BO_3)_4:Eu^{3+}/Tb^{3+}$ (RE=Y, Gd) phosphors from sol–gel composition of hybrid precursors, Solid State Sciences 10 (2008) 82–89.
[16] B. Yue, J. Gu, G. Yin, Z. Huang, X. Liao, Y. Yao, Y. Kang, P. You, Preparation and properties of the green-emitting phosphors $NaCa_{0.98-x}Mg_xPO_4$:Eu2+0:02, Current Applied Physics 10 (2010) 1216–1220.
[17] F. Lei, B. Yan, Hydrothermal synthesis and luminescence of $CaMO_4:RE^{3+}$ (M=W, Mo; RE=Eu, Tb) submicro-phosphors 181 (2008) 855–862Journal of Solid State Chemistry 181 (2008) 855–862.
[18] K. Vivekanandan, S. Selvasekarapandian, P. Kolandaivel, M.T. Sebastian, S. Suma, Raman and FT-IR spectroscopic characterization of flux grown $KTiOPO_4$ and $KRbTiOPO_4$ non-linear optical crystals, Materials Chemistry and Physics 49 (1997) 204–210.
[19] Y. Huang, X. Wang, H.S. Lee, E. Cho, K. Jang, Y. Tao, Synthesis, vacuum ultraviolet and ultraviolet spectroscopy of Ce^{3+} ion doped olgite Na (Sr, Ba)PO_4 40 (2007) 7821–7825Journal of Physics D: Applied Physics 40 (2007) 7821–7825.
[20] R.L. Frost, J. Cejka, M. Weier, A Raman spectroscopic study of the uranyl phosphate mineral threadgoldite, Spectrochimica Acta A 65 (2006) 797–801.
[21] T. Rojac, O. Masson, R. Guinebreti'ere, M. Kosec, B. Malǐc, J. Holc, A study of the mechanochemical synthesis of $NaNbO_3$, Journal of the European Ceramic Society 27 (2007) 2265–2271.
[22] J. Jeong, V.R. Bandi, B.K. Grandhe, K. Jang, H.S. Lee, Photoluminescence characteristics of reddish-orange Eu^{3+} or Sm^{3+} singly-doped and Eu^{3+} and Sm^{3+} co-doped $KZnGd(PO4)_2$ phosphors, Journal of the Korean Physical Society 58 (2) (2011) 306–310.
[23] M. Peng, Z. Pei, G. Hong, Q. Su, The reduction of Eu^{3+} to Eu^{2+} in $BaMgSiO_4$:Eu prepared in air and the luminescence of $BaMgSiO_4:Eu^{2+}$ phosphor, Journal of Materials Chemistry 13 (2003) 1202–1205.
[24] M. Grinberg, J. Barzowska, A. Baran, B. Kukliński, Characterization of various Eu^{2+} sites in $Ca_2SiO_4:Eu^{2+}$ and $Ba_2SiO_4:Eu^{2+}$ by high-pressure spectroscopy, Materials Science Poland 29 (4) (2011) 272–277, http://dx.doi.org/10.2478/s13536-011-0038-0.
[25] J. Gu, B. Yue, G. Yin, X. Liao, Z. Huang, Y. Yao, Y. Kang, A novel blue emitting phosphor $NaBa_{0.98}Eu_{0.02}PO_4$ and the improvement of its luminescence properties, Frontiers of Materials Science in China 4 (1) (2010) 90–94.
[26] B.K. Grandhe, V.R. Bandi, K. Jang, S. Ramaprabhu, S. Yi, J. Jeong, Enhanced red emission from $YVO_4:Eu^{3+}$ nano phosphors prepared by simple co-precipitation method, Electronic Materials Letters 7 (2) (2011) 161–165.
[27] S.S. Yao, L.H. Xue, Y.W. Yan, Synthesis and luminescent properties of hexagonal $BaZnSiO_4:Eu^{2+}$ phosphor, Applied Physics B 102 (2011) 705–709.
[28] B. Liu, Y. Wang, J. Zhou, F. Zhang, Z. Wang, The reduction of Eu^{3+} to Eu^{2+} in $BaMgAl_{10}O_{17}$:Eu and the photoluminescence properties of $BaMgAl_{10}O_{17}:Eu^{2+}$ phosphor, Journal of Applied Physics 106 (2009) 053102.
[29] R.D. Shannon, Revised effective ionic radii and systematic studies of interatomic distances in halides and chaleogenides, Acta Crystals, A 32 (1976) 751–767.
[30] M. Peng, Z. Pei, G. Hong, Q. Su, Study on the reduction of $Eu^{3+} \rightarrow Eu^{2+}$ in $Sr_4Al_{14}O_{25}$:Eu prepared in air atmosphere, Chemistry and Physics Letters 371 (2003) 1–6.
[31] G.B. Kumar, S. Buddhudu, Synthesis and emission analysis of RE^{3+} (Eu^{3+} or Dy^{3+}):Li_2TiO_3 ceramics, Ceramics International 35 (2009) 521–525.
[32] X. Sun, J. Zhang, X. Liu, L. Lin, Enhanced luminescence of novel $Ca_3B_2O_6:Dy^{3+}$ phosphors by Li^+-codoping for LED applications, Ceramics International 38 (2012) 1065–1070.
[33] R. Ghildiyal, C.H. Hsu, C.H. Lu, Aliovalent ion substitution and enhanced photoluminescence of $Sr_2SiO_4:Tb^{3+}/Z^+$ (Z=Li, Na, and K) phosphors, International Journal of Applied Ceramic Technology 8 (4) (2011) 759–765.